AJNR

Prediction of Carotid Intraplaque Hemorrhage Using Adventitial Calcification and Plaque Thickness on CTA

L.B. Eisenmenger, B.W. Aldred, S.-E. Kim, G.J. Stoddard, A. de Havenon, G.S. Treiman, D.L. Parker and J.S. McNally

Prediction of Carotid Intraplaque Hemorrhage Using Adventitial Calcification and Plaque Thickness on CTA

L.B. Eisenmenger, B.W. Aldred, S.-E. Kim, G.J. Stoddard, A. de Havenon, G.S. Treiman, D.L. Parker, and J.S. McNally

ABSTRACT

BACKGROUND AND PURPOSE: Carotid intraplaque hemorrhage is associated with stroke, plaque thickness, stenosis, ulceration, and adventitial inflammation. Conflicting data exist on whether calcification is a marker of plaque instability, and no data exist on adventitial calcification. Our goal was to determine whether adventitial calcification and soft plaque (a rim sign) help predict carotid intraplaque hemorrhage.

MATERIALS AND METHODS: This was a retrospective cohort study of 96 patients who underwent carotid MRA and CTA within 1 month, from 2009 to 2016. We excluded occlusions ($n = 4$) and near occlusions ($n = 0$), leaving 188 carotid arteries. Intraplaque hemorrhage was detected by using MPRAGE. Calcification, adventitial pattern, stenosis, maximum plaque thickness (total, soft, and hard), ulceration, and intraluminal thrombus on CTA were recorded. Atherosclerosis risk factors and medications were recorded. We used mixed-effects multivariable Poisson regression, accounting for 2 vessels per patient. For the final model, backward elimination was used with a threshold of $P < .10$. Receiver operating characteristic analysis determined intraplaque hemorrhage by using the area under the curve.

RESULTS: Our final model included the rim sign (prevalence ratio = 11.9, $P < .001$) and maximum soft-plaque thickness (prevalence ratio = 1.2, $P = .06$). This model had excellent intraplaque hemorrhage prediction (area under the curve = 0.94), outperforming the rim sign, maximum soft-plaque thickness, NASCET stenosis, and ulceration (area under the curve = 0.88, 0.86, 0.77, and 0.63, respectively; $P < .001$). Addition of the rim sign performed better than each marker alone, including maximum soft-plaque thickness (area under the curve = 0.94 versus 0.86, $P < .001$), NASCET stenosis (area under the curve = 0.90 versus 0.77, $P < .001$), and ulceration (area under the curve = 0.90 versus 0.63, $P < .001$).

CONCLUSIONS: The CTA rim sign of adventitial calcification with internal soft plaque is highly predictive of carotid intraplaque hemorrhage.

ABBREVIATIONS: AUC = area under the curve; IPH = intraplaque hemorrhage; ROC = receiver operating characteristic

Carotid atherosclerotic plaque contributes to 10%–15% of ischemic strokes in the United States.[1] MR imaging–detected carotid intraplaque hemorrhage (IPH) is an accepted marker of plaque instability and stroke risk independent of stenosis, with an annual stroke rate as high as 45% in patients with >50% stenosis and IPH.[2-5] Carotid IPH can be detected with heavily T1-weighted sequences, including the MPRAGE sequence, which can discriminate between IPH and lipid/necrotic core.[6] MPRAGE is superior in detecting IPH compared with conventional MR imaging sequences, with higher sensitivity, specificity, and interrater reliability compared with 3D TOF or FSE T1WI sequences.[7]

Lumen markers have been linked to IPH, including stenosis, plaque thickness, and ulceration. These markers can be detected

by CTA. IPH is known to increase in prevalence with increasing lumen stenosis.[8] Additional studies have suggested that CTA-detected ulceration can be used as a surrogate marker for IPH.[9] Plaque thickness has also recently been associated with high plaque signal on 3D TOF imaging, attributed to IPH.[10,11] Recently, we found that these markers in combination (plaque thickness, millimeter stenosis, and ulceration) allow optimal discrimination of IPH in a model including the clinical factors of age and male sex.[12] Together these factors may provide clues to the pathogenesis of IPH.

Most recently, studies have linked IPH with adventitial inflammation and microvessel permeability detectable by using dynamic contrast-enhanced MR imaging.[8,13] Adventitial inflammation and oxidative stress have also been linked to endothelial bone-morphogenic proteins,[14] suggesting that adventitial calcification may also represent a marker of adventitial inflammation[15]; however, this has not yet been investigated in the setting of IPH. Vascular calcification is often seen with carotid plaque, though conflicting data exist in relation to plaque vulnerability. One study of 30 patients found that fibrous cap inflammation more often occurs in noncalcified than in calcified plaques, suggesting that calcification indicates plaque stability.[16] An additional study of patients with symptomatic plaques (recent TIA, stroke, or amaurosis fugax) versus asymptomatic patients with critical stenosis found that the percentage of plaque calcification area was 2-fold greater in asymptomatic-versus-symptomatic plaques, and there was an inverse relationship between calcification and macrophage infiltration.[17] A different study investigating 611 carotid plaques by CT and MR imaging found that larger calcification volume was associated with higher IPH prevalence and a lower lipid core prevalence, suggesting that calcification may not be a stabilizing factor.[18] However, these studies evaluated total calcification volume or its binary presence or absence, and adventitial calcification coupled with soft plaque has not yet been addressed, to our knowledge.

Because IPH is becoming more clinically relevant in identifying cryptogenic stroke sources[19] and IPH indicates a medically refractory population with high future stroke risk,[4] prediction models are greatly needed in patients undergoing alternate imaging such as CTA. Of clinical relevance, a CTA-IPH prediction model would be especially useful in patients with contraindications to MR imaging (eg, with pacemakers) or as a cost-saving measure to prevent unneeded MR imaging in patients with very high or very low likelihood of IPH. Current prediction models discussed above based on plaque thickness, stenosis, and ulceration leave room for improvement. Because adventitial inflammation is highly associated with IPH and chronic inflammation is associated with calcification, this study was undertaken to determine whether adventitial calcification with internal soft plaque (a rim sign) could aid in carotid IPH prediction. Our hypothesis was that the rim sign may help predict carotid IPH compared with standard markers, including soft-plaque thickness, stenosis, or ulceration alone.

MATERIALS AND METHODS
Clinical Study Design
Institutional review board approval was obtained for this retrospective cohort study from 2009 to 2016 in patients who underwent both CTA and MRA work-up of carotid disease at the University Medical Center and VA Medical Center in Salt Lake City, Utah. Due to the retrospective nature, informed consent was not required by the institutional review board. The only inclusion criteria were MRA and CTA performed within 1 month in the same patient within the study timeframe. Ninety-six patients qualified for the study, with 192 carotid arteries. Exclusions included carotid occlusions ($n = 4$) and near occlusions ($n = 0$) because lumen markers are difficult or impossible to determine in these cases. No vessels underwent carotid surgery or stent placement between scans. One hundred eighty-eight carotid arteries were left in the final analysis. Although a few scans exhibited mild motion artifacts primarily from swallowing, no carotid images were sufficiently limited to be excluded from interpretation.

MR Imaging Protocol
Images were obtained on 1.5 and 3T MR imaging scanners (Trio, Verio, and Prisma; Siemens, Erlangen, Germany) with standard or custom carotid coils.[20] Our standard clinical MRA protocol includes axial TOF, axial MPRAGE, coronal precontrast, postcontrast arterial, and venous phase T1-weighted images. Coronal postcontrast MRA neck images extended from the aortic arch through the circle of Willis.

IPH Determination by MPRAGE
Our prior research has shown that MPRAGE images have high intra- and interobserver agreement at both field strengths, with or without specialized coils, and that the MPRAGE-positive area highly correlates with the IPH area on histology.[6] MPRAGE parameters included the following: 3D, TR/TE/TI = 6.39/2.37/370 ms, flip angle = 15°, FOV = 130 × 130 × 48 mm^3, matrix = 256 × 256 × 48, voxel = 0.5 × 0.5 × 1.0 mm^3, fat saturation, acquisition time ~ 5 minutes. Images were obtained from 20 mm below to 20 mm above the carotid bifurcation at a 1.0-mm section thickness.[21] To produce 3D images, we used a secondary phase-encoding gradient in the section-select direction, and measurements for all section-selection phase encodings were performed with rapid acquisition in each segment. Carotid IPH was determined by MPRAGE-positive plaque with at least 1 voxel demonstrating at least 2-fold higher signal intensity relative to adjacent sternocleidomastoid muscle as previously described.[6]

CTA Protocol
CTA was performed with a 64-section scanner (Definition or Definition AS; Siemens), with dose modulation and 100–120 kV-(peak). Images were obtained from the aortic arch through the skull vertex at a thickness of 0.625 mm. Intravenous access was through an antecubital vein by using an 18- or 20-ga angiocatheter. A total of 100 mL of iopamidol (Isovue 370; Bracco, Princeton, New Jersey) was injected at 4 mL/s. Bolus monitoring used an ROI in the ascending aorta and a trigger at 100 HU. Injections were performed with a 10-second delay. Multiplanar reformats were created, and images were reviewed on a PACS workstation on CTA settings (window 96, level 150 HU) and were modified as required to depict CTA lumen markers and calcification.

Imaging Reviewers

All carotid imaging markers were determined by consensus of 2 reviewers blinded to stroke status and clinical covariates. In cases of disagreement, consensus was obtained with a third reviewer. CTA lumen and calcification markers were determined separately, and reviewers were blinded to MR imaging IPH status. All reviewers had experience with neurovascular imaging interpretation and included a radiology resident in training (L.B.E.), neuroradiology fellow (B.W.A.), and board-certified neuroradiology attending physician (J.S.M.). κ analysis was performed to determine the rim sign interrater reliability (0.85) and intrarater reliability (0.86). CTA calcification examples are shown in Figs 1 and 2.

CTA Markers

CTA markers included the time between MR imaging and CTA, presence of calcification, adventitial calcification pattern, per-

FIG 1. Positive rim sign and carotid IPH. Top: Carotid CTA with positive rim signs (*arrows*) in both carotid plaques. Bottom: MPRAGE with bilateral carotid IPH (*arrows*) in the same patient. IPH was defined by MPRAGE-positive plaque, using a signal threshold of 2-fold signal intensity over the adjacent sternocleidomastoid muscle.

centage diameter stenosis, millimeter stenosis, maximum total plaque thickness, maximum soft-plaque thickness, maximum hard-plaque thickness, ulceration, and intraluminal thrombus. All measurements were obtained by using the submillimeter tool on a PACS workstation.

Time between CTA and MR Imaging

The time between scans was recorded in days and was used as a potential confounder for the association between CTA markers and MR imaging–detected IPH.

CTA Calcification Markers

Carotid arteries with thin adventitial calcification of <2 mm were subdivided into 2 groups: A positive rim sign was defined as adventitial calcification (<2-mm thick) with internal soft plaque (≥2-mm thickness), and a negative rim sign was defined as adventitial calcification (<2-mm thick) with minimal if any internal soft plaque (<2-mm thickness). "Bulky calcification" was defined as calcification measuring ≥2-mm thick without associated thin adventitial calcification measuring <2-mm thick.

CTA Lumen Markers

Percentage diameter stenosis was determined by using NASCET criteria on contrast CTA. Briefly, the diameter (b) at the level of maximal stenosis and diameter (a) of the ICA distal to the stenosis were used to calculate percentage diameter stenosis by using the formula $[(a - b) / a] \times 100\%$. Carotid stenosis was measured at the narrowest segment of the carotid plaque (b) on axial images, perpendicular to the long axis of the vessel on multiplanar reformats by using a submillimeter measurement tool on a PACS workstation. The distal ICA diameter (a) was measured beyond the bulb where the walls are parallel and no longer tapering per NASCET criteria.[22-24] We performed the multivariable regression analysis by using both the NASCET measurement of percentage diameter stenosis $[(a - b) / a] \times 100\%$ and the previously described millimeter stenosis (b) measurement.[25] Near occlusions were excluded from percentage stenosis calculation and were identified by the following CTA criteria: visible bulb stenosis, distal ICA diameter of ≤3 mm, and distal ICA/distal external carotid artery ratio of ≤1.25 originally adapted from standard conven-
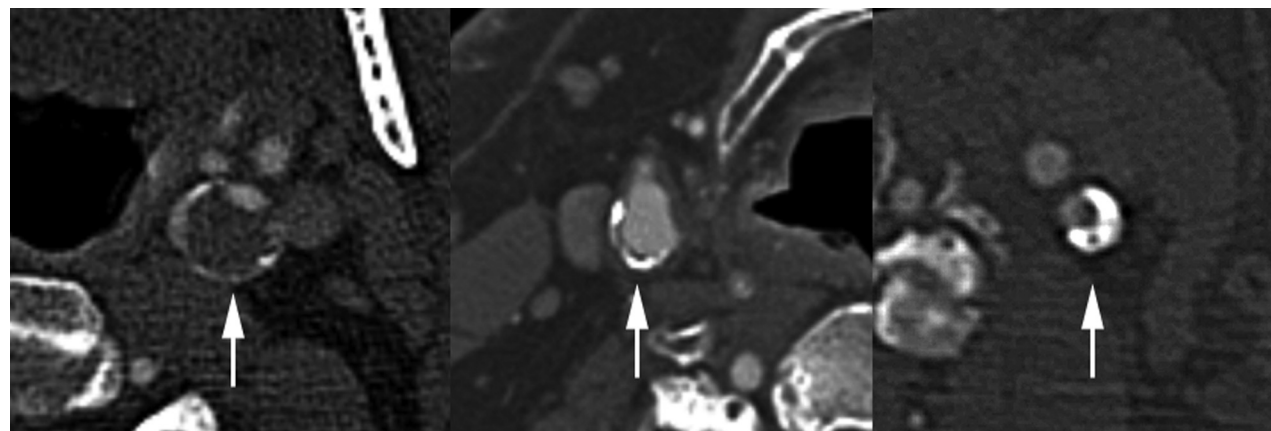
FIG 2. CTA calcification. Left: Positive rim sign (*arrow*), adventitial calcification measuring <2 mm in thickness with adjacent soft plaque measuring ≥2 mm in thickness. Middle: Adventitial calcification without a rim sign (*arrow*), adventitial calcification measuring <2 mm in thickness with <2 mm adjacent soft plaque. Right: Bulky calcification (*arrow*), calcified plaque of ≥2 mm.

tional angiography.[24,25] The presence of ulceration was determined on CTA images by using a size threshold of 2 mm reported in prior studies.[9] Intraluminal thrombus was defined by an intraluminal filling defect on CTA as previously described.[26] Maximum plaque thickness was measured in the transverse plane on CTA. These CTA lumen markers are shown in the On-line Fig 1. In addition, maximum soft-plaque and hard-plaque thicknesses were measured on CTA, as previously described.[27]

Clinical Demographics

Clinical demographics were determined by retrospective chart review. Carotid atherosclerosis risk factors of age, male sex, diabetes, hypertension, hyperlipidemia, body mass index, and smoking status were identified. These were determined by retrospective chart review, with standard clinical definitions. For hypertension, the diagnosis was made when the average of ≥2 diastolic blood pressure measurements on at least 2 subsequent visits was ≥90 mm Hg or when the average of multiple systolic blood pressure readings on ≥2 subsequent visits was ≥140 mm Hg. For hyperlipidemia, the diagnosis was made when low-density lipoprotein was >100 mg/dL. Cardiovascular medications were recorded, including antiplatelets, anticoagulants, statins, and antihypertensives.

Statistical Analysis

Intrarater (test-retest) reliability for the presence of the rim sign was assessed for 1 reviewer (J.S.M.), and interrater reliability for the presence of the rim sign was assessed for 2 reviewers (J.S.M. and L.B.E.), both with a κ coefficient. Statistical modeling was performed by using generalized estimating equations to account for data clustering, with up to 2 carotid arteries per patient. Carotid arteries were treated as separate units or units of analysis grouped within each subject because IPH may be associated with local markers of carotid plaque vulnerability (plaque calcification pattern, thickness, stenosis, and other lumen markers). At the patient level, systemic clinical factors affecting both carotid arteries (age, male sex, and other cardiovascular risk factors and medications) were considered in the model as potential confounding variables. Given that >1 marker for IPH was being studied, potential confounding was investigated on the outcome variable or groups positive and negative for IPH, so only 1 data table was required, with P values from univariable generalized estimating equation Poisson regression models. The Poisson regression approach directly estimates the risk ratio, or prevalence ratio in our case, which is more intuitive to interpret than an odds ratio from a logistic regression approach.[28] Next, all potential confounding variables with $P < .10$ from a univariable model were placed in an initial multivariable generalized estimating equation Poisson regression model for IPH and then were eliminated in a backward fashion until all remaining variables met the threshold $P < .10$. Liberal significance criteria, $P < .10$, were used to protect against residual confounding.[29]

For hypothesis testing of which markers are predictive of IPH, we used the traditional $P < .05$. In binary outcome models, 5 outcome events for every predictor variable are sufficient to avoid overfitting.[30] With 44 carotid IPH events and 144 non-IPH events, 44/5 = 8.8, or up to 8 predictor variables could be included

Table 1: Clinical characteristics

Characteristic	Patients (N = 96)
Age (mean) (SD) (yr)	65.7 (13.4)
Male sex (No.) (%)	75 (78.1)
BMI (mean) (SD) (kg/m²)	28.0 (4.9)
Smoking (No.) (%)	
Current smoker	28 (29.2)
Prior smoker	24 (25.0)
Hypertension (No.) (%)	75 (78.1)
Hyperlipidemia (No.) (%)	61 (64.2)
Diabetes (No.) (%)	38 (39.6)
Antihypertension (No.) (%)	60 (62.5)
Statins (No.) (%)	50 (52.1)
Antiplatelets (No.) (%)	50 (52.1)
Anticoagulation (No.) (%)	9 (9.4)
Days between CTA and MRA (mean) (SD)	5.9 (8.6)

Note:—BMI indicates body mass index.

in the model without overfitting, exceeding the number of variables remaining in the final model. To assess the discriminatory potential of each marker or combination of markers, we reported clustered data area under the receiver operating characteristic (ROC) curve (AUC), with bootstrapped 95% confidence intervals.[31] Similarly, AUCs were compared by using the clustered method of Pepe et al.[31] To guard against overfitting and optimism of the AUCs, in which an AUC could be higher in the present sample of patients than it would in future patients, we performed a bootstrap validation for each clustered data AUC calculation on the fixed list of predictors in the model.[32] Given that in all cases the optimism was <1%, so that the original AUCs and bootstrapped validated AUCs were identical to the precision reported, there was no need to report both. All statistical analyses were performed with STATA 13.1 statistical software (StataCorp, College Station, Texas).

RESULTS

Clinical Characteristics

Ninety-six patients were recruited for the study. Patients were predominantly older men (mean age, 65.7 ± 13.4 years; 78.1% male) with carotid atherosclerosis risk factors (54.2% were current or prior smokers, 78.1% had hypertension, 64.2% had hyperlipidemia, 39.6% had diabetes), and many were on medical therapy for carotid disease (62.5% on antihypertensives, 52.1% on statins, 52.1% on antiplatelets) (Table 1).

Imaging and Clinical Characteristics by Vessel

We evaluated imaging and clinical characteristics by vessel in groups positive and negative for IPH in Table 2. Each patient contributed 2 carotid arteries, with the exception of 4 carotid occlusions, leaving 188 carotid arteries for the final sample. Carotid stenosis was worse in the group positive for IPH versus the negative one (NASCET stenosis of 53.5% versus 24.9% and millimeter stenosis of 2.27 versus 3.60 mm, $P < .001$). Maximum plaque thickness was also higher in the group positive for IPH versus the negative one (5.93 versus 3.42 mm, $P < .001$), as was maximum soft-plaque thickness (5.26 versus 2.99 mm, $P < .001$) and maximum hard-plaque thickness (2.97 versus 1.91 mm, $P = .002$). There was higher prevalence of plaque ulceration (56.8% versus 29.9%, $P = .005$) and intraluminal thrombus, though this was rare and not significantly different between the 2 groups

Table 2: Carotid plaque CTA markers associated with IPH[a]

Imaging and Clinical Characteristics by Vessel	IPH (−) (n = 144)	IPH (+) (n = 44)	P Value
Carotid NASCET percentage stenosis (mean) (SD)	24.9 (29.5)	53.5 (24.5)	<.001
Mild (0%–49.9%) (No.) (%)	112 (77.8)	16 (36.4)	
Moderate (50%–69.9%) (No.) (%)	16 (11.1)	14 (31.8)	
Severe (70%–99.9%) (No.) (%)	16 (11.1)	14 (31.8)	
Carotid mm stenosis (mean) (SD)	3.60 (1.47)	2.27 (1.21)	<.001
Carotid maximum total plaque thickness (mean) (SD) (mm)	3.42 (1.83)	5.93 (1.48)	<.001
Carotid maximum soft-plaque thickness (mean) (SD) (mm)	2.99 (1.60)	5.26 (1.50)	<.001
Carotid maximum hard-plaque thickness (mean) (SD) (mm)	1.91 (1.72)	2.97 (1.18)	.002
Carotid plaque ulceration (No.) (%)	43 (29.9)	25 (56.8)	.005
Carotid intraluminal thrombus (No.) (%)	11 (7.6)	6 (13.6)	.185
Carotid calcification present (No.) (%)	103 (71.5)	43 (97.7)	.015
Bulky calcification (≥2 mm) (No.) (%)[b]	66 (45.8)	36 (81.8)	.001
Thin adventitial calcification (<2 mm)			
Rim sign + (No.) (%)	17 (11.8)	39 (88.6)	<.001
Rim sign − (No.) (%)	60 (41.7)	4 (9.1)	<.001
Days between MRA and CTA (No.) (SD)	5.6 (8.2)	6.9 (9.3)	.453
Male sex (No.) (%)	103 (71.5)	43 (97.7)	.017
Age (mean) (SD) (yr)	63.4 (14.1)	73.5 (7.2)	<.001
BMI (mean) (SD) (kg/m^2)	28.0 (5.2)	28.1 (4.2)	.955
Smoking (No.) (%)			
Current smoker	49 (34.0)	4 (9.1)	.019
Prior smoker	34 (23.6)	13 (29.6)	.534
Hypertension (No.) (%)	110 (76.4)	37 (84.1)	.382
Hyperlipidemia (No.) (%)	88 (61.1)	33 (78.6)	.092
Diabetes (No.) (%)	50 (34.7)	24 (54.6)	.057
Antihypertension (No.) (%)	85 (59.0)	33 (75.0)	.143
Statin (No.) (%)	68 (47.2)	29 (65.9)	.080
Antiplatelets (No.) (%)	69 (47.9)	27 (61.4)	.206
Anticoagulation (No.) (%)	13 (9.0)	5 (11.4)	.713

Note:—IPH (−) indicates no MPRAGE positive plaque, and IPH absence; IPH (+), MPRAGE positive plaque, and IPH presence. Bulky calcification indicates calcified plaque of ≥2 mm. Two types of adventitial calcification were recorded, both with <2-mm adventitial calcification: Rim sign −, <2-mm soft plaque; Rim sign +, ≥2mm soft plaque.
[a] From the 96 patients, 188 carotid arteries were analyzed after excluding occlusions (n = 4) and near occlusions (n = 0). Means/SDs were calculated using ordinary formulas. We based significance tests and P values on univariable generalized estimating equation Poisson regression, taking into account the correlation of up to 2 carotid arteries per person. Factors with P < .10 were included in the initial multivariable Poisson regression analysis.

Table 3: Final model of CTA markers associated with IPH[a]

Carotid IPH Prediction	PR	P Value	95% CI
Carotid plaque rim sign (present versus absent)	11.9	<.001	4.4–32.0
Maximum soft-plaque thickness (per 1-mm increase)	1.2	.06	0.99–1.40

Note:—PR indicates prevalence ratio.
[a] After multivariable Poisson regression with sequential backward elimination of factors that did not meet the threshold of P < .10, the final carotid IPH model depended on the positive rim sign and maximum soft-plaque thickness.

(13.6% versus 7.6%, P = .185). Some factors were potential confounders between groups positive and negative for IPH (P < .10), requiring multivariable regression.

Multivariable Generalized Estimating Equation Poisson Regression Analysis

Multivariable regression analysis was performed with the outcome of carotid IPH and the primary predictor, the rim sign. Potential confounders were eliminated in a backward fashion with a threshold of P > .10. At this threshold, CTA predictors of IPH included the rim sign (prevalence ratio = 11.9; 95% CI, 4.4–32.0; P < .001) and maximum soft-plaque thickness (prevalence ratio = 1.2; 95% CI, 0.99–1.40; P = .06) (Table 3).

IPH ROC Comparison Analysis

ROC comparison analysis for IPH is shown in Fig 3. The final IPH prediction model was excellent in determining carotid IPH (AUC = 0.94; 95% CI, 0.90–0.97). The final model performed significantly better than the rim sign alone (AUC = 0.94 versus 0.88, P < .001), maximum soft-plaque thickness alone (AUC = 0.94 versus 0.86, P < .001), NASCET stenosis alone (AUC = 0.94 versus 0.77, P < .001), and ulceration alone (AUC = 0.94 versus 0.63, P < .001) (Fig 3A). In addition, IPH prediction with-versus-without the rim sign was significantly better in models using maximum soft-plaque thickness (AUC = 0.94 versus 0.86, P < .001), NASCET stenosis (0.90 versus 0.77, P < .001), or ulceration (0.90 versus 0.63, P < .001).

DISCUSSION

Carotid MR imaging optimally detects carotid stroke sources and future stroke risk by characterizing IPH.[2-5] Major barriers to progress are that the pathophysiology of carotid IPH is unknown and there are no known treatments or preventative measures available. Another barrier is that many patients undergo other imaging, including CTA, during work-up, and IPH status is unknown without additional MR imaging with its associated costs and contraindications (eg, pacemaker). Our study shows that of the CTA markers predicting IPH, adventitial calcification with internal soft plaque, a rim sign, performs best. Identifying IPH by using CTA markers would greatly benefit clinicians. IPH status can identify stroke sources that would otherwise be ignored and diagnosed as cryptogenic if stenosis is <50%.[19] In addition, IPH is known to be refractory to standard medical management with an up to 45% annual stroke risk in patients with >50% stenosis.[4] Identification of carotid IPH is becoming more and more clinically relevant, indicating the need for early optimal medical therapy, close follow-up intervals for stenosis progression or new ischemic stroke symptoms, and identification of patients with treatment failure necessitating surgery or stent placement.

The underlying mechanism behind this association of IPH and the rim sign is uncertain. A potential link between IPH and adventitial pathology may lie with adventitial neovessel proliferation and inflammation.[8] Adventitial inflammation and oxidative stress have been linked to endothelial bone-morphogenic pro-
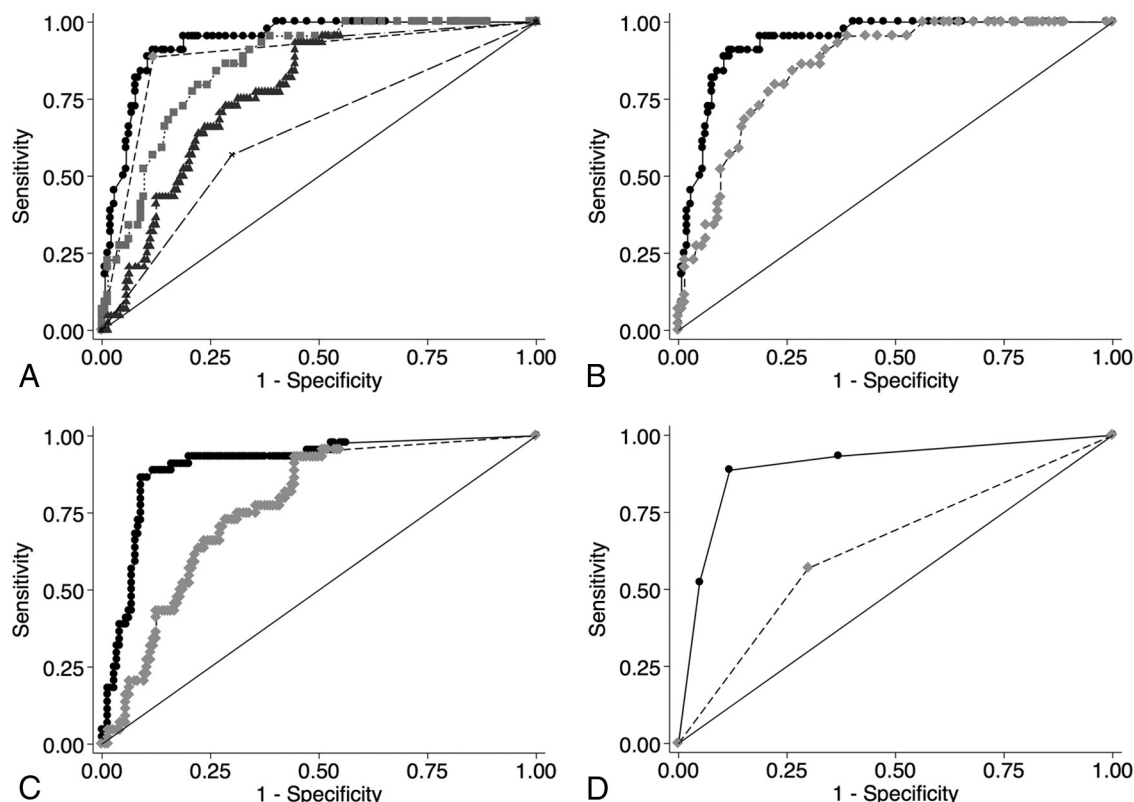
FIG 3. *A*, ROC comparison analysis demonstrates the superiority of the final model (rim sign and maximum soft-plaque thickness) in predicting carotid IPH. 1) Rim sign + maximum soft-plaque thickness (*black circles*). The *solid line* indicates AUC = 0.94 (95% CI, 0.90–0.97). 2) Rim sign (*light gray diamonds*). The *dashed line* indicates AUC = 0.88, (95% CI, 0.83–0.94). 3) Maximum soft-plaque thickness (*light gray squares*). The *dotted line* indicates AUC = 0.86 (95% CI, 0.80–0.91). 4) NASCET stenosis (*dark gray triangles*). The *dashed-dotted line* indicates AUC = 0.77 (95% CI, 0.70–0.84). 5) Ulceration (*x*). The *large dashed line* indicates AUC = 0.63, (95% CI, 0.55–0.72). *B*, ROC comparison of the rim sign in addition to maximum soft-plaque thickness in predicting IPH. 1) Rim sign + maximum soft-plaque thickness (*black circles*). The *solid line* indicates AUC = 0.94 (95% CI, 0.90–0.97). 2) Maximum soft-plaque thickness (*light gray diamonds*). The *dotted line* indicates AUC = 0.86, (95% CI, 0.80–0.91) (*P* < .001). *C*, ROC comparison of the rim sign in addition to NASCET stenosis in predicting IPH. 1) Rim sign + NASCET stenosis (*black circles*). The *solid line* indicates AUC = 0.90 (95% CI, 0.85–0.96). 2) NASCET stenosis (*light gray diamonds*). The *dotted line* indicates AUC = 0.77 (95% CI, 0.70–0.84) (*P* < .001). *D*, ROC comparison of the rim sign in addition to ulceration in predicting IPH. 1) Rim-sign + ulceration (*black circles*). The *solid line* indicates AUC = 0.90 (95% CI, 0.84–0.96). 2) Ulceration (*light gray diamonds*). The *dotted line* indicates AUC = 0.63 (95% CI, 0.55–0.72) (*P* < .001).

tein-4 production by endothelial cells.[14] IPH has also been shown to be stimulated by the angiotensin pathway in animal models,[33] and blockade of the angiotensin system inhibits vascular calcification by suppressing bone-morphogenic protein-2.[34] Bone-morphogenic protein-4 and bone-morphogenic protein-2 are known to stimulate pathways leading to vascular calcification, with interactions among endothelial cells, macrophages, and pericytic myofibroblasts forming a vascular osteogenic triad.[14] The rim sign of adventitial calcification may therefore be a marker of adventitial neovessel dysfunction and hemorrhage propensity.

Our study also shows not only that IPH prevalence is high with a rim sign but that it further increases with increasing soft-plaque thickness. This finding corresponds with prior research demonstrating a high ROC AUC by using soft-plaque thickness to predict high plaque signal on 3D TOF, though this was only assessed in severe stenosis groups.[10,11] Further research has demonstrated that soft-plaque thickness on CTA is highly predictive of carotid IPH on T1WI sequences.[27] One limitation of these prior studies was that TOF and other T1-weighted images have poor sensitivity and specificity compared with the MPRAGE sequence.[7] Most important, our study confirms this high association of IPH with

soft-plaque thickness. This association is not surprising because IPH is known to stimulate plaque growth with time.[35] Larger plaques may be inherently more unstable and prone to hemorrhage, potentially due to a larger lipid-rich core and/or a higher number or more permeable plaque neovessels.

Most interesting, some factors did not remain in our final model for carotid IPH. One of these factors, stenosis (NASCET percentage or millimeter), was associated with IPH on univariable analysis but did not significantly contribute to IPH after multivariable regression. While initial reports found that stenosis was associated with IPH,[8] we have recently shown that stenosis alone is a poor discriminator of IPH compared with multivariable models combining plaque markers and clinical markers.[12] In addition, prior research indicates that plaque ulceration may be used as a surrogate marker for IPH.[9] However, our current study shows that ulceration was a poor predictor of IPH, performing worse than NASCET stenosis. The relatively poor prediction of IPH by using ulceration is in line with predictions by other groups.[27] Our data add to previous studies on soft-plaque thickness by finding additional IPH discrimination by using the rim sign, with significantly higher ROC curves.

Because there was varied time between MR imaging and CTA in this retrospective study, we elected to exclude patients with >1 month between scans. In data not shown, we found that the association between the CTA rim sign and IPH remained high even in patients with CTA and MRA scans separated by months to years. This outcome suggests that carotid IPH may continue for long periods, an observation supported by multiple prior studies showing MR imaging IPH signal persisting for months to years.[35-38]

A limitation of our study is related to the narrow population undergoing stroke work-up, limiting generalizability to the population as a whole. Still, this is the population often undergoing CTA to determine stroke etiology based on stenosis, and our results may help determine IPH status and further refine stroke risk in this important group.[3-5] Finally, while this study is limited due to its retrospective nature and inability to determine causation, these data add further support to the ability of CTA to suggest the presence or absence of IPH with a high level of discrimination. Future prospective studies could test whether adventitial calcification and plaque thickness precede IPH or vice versa.

CONCLUSIONS

Carotid IPH can be highly predicted by CTA markers, including the rim sign of adventitial calcification and internal soft plaque. Because CTA is often used in patients undergoing stroke work-up, a rim sign combined with soft-plaque thickness may identify carotid stroke sources that would otherwise be ignored using lumen stenosis or ulceration. The rim sign could also be used to identify patients with a high likelihood of having IPH, to enrich recruitment for future studies aimed at preventing stroke in this high-risk population.

REFERENCES

1. Go AS, Mozaffarian D, Roger VL, et al; American Heart Association Statistics Committee and Stroke Statistics Subcommittee. **Heart Disease and Stroke Statistics: 2013 update—a report from the American Heart Association.** *Circulation* 2013;127:e6–e245 CrossRef Medline
2. Treiman GS, McNally JS, Kim SE, et al. **Correlation of carotid intraplaque hemorrhage and stroke using 1.5 T and 3 T MRI.** *Magn Reson Insights* 2015;8(suppl 1):1–8 CrossRef Medline
3. Saam T, Hetterich H, Hoffmann V, et al. **Meta-analysis and systematic review of the predictive value of carotid plaque hemorrhage on cerebrovascular events by magnetic resonance imaging.** *J Am Coll Cardiol* 2013;62:1081–91 CrossRef Medline
4. Hosseini AA, Kandiyil N, Macsweeney ST, et al. **Carotid plaque hemorrhage on magnetic resonance imaging strongly predicts recurrent ischemia and stroke.** *Ann Neurol* 2013;73:774–84 CrossRef Medline
5. Gupta A, Baradaran H, Schweitzer AD, et al. **Carotid plaque MRI and stroke risk: a systematic review and meta-analysis.** *Stroke* 2013;44:3071–77 CrossRef Medline
6. McNally JS, Yoon HC, Kim SE, et al. **Carotid MRI detection of intraplaque hemorrhage at 3T and 1.5T.** *J Neuroimaging* 2015;25:390–96 CrossRef Medline
7. Ota H, Yarnykh VL, Ferguson MS, et al. **Carotid intraplaque hemorrhage imaging at 3.0-T MR imaging: comparison of the diagnostic performance of three T1-weighted sequences.** *Radiology* 2010;254:551–63 CrossRef Medline
8. Sun J, Song Y, Chen H, et al. **Adventitial perfusion and intraplaque hemorrhage: a dynamic contrast-enhanced MRI study in the carotid artery.** *Stroke* 2013;44:1031–36 CrossRef Medline
9. U-King-Im JM, Fox AJ, Aviv RI, et al. **Characterization of carotid plaque hemorrhage: a CT angiography and MR intraplaque hemorrhage study.** *Stroke* 2010;41:1623–29 CrossRef Medline
10. Gupta A, Baradaran H, Mtui EE, et al. **Detection of symptomatic carotid plaque using source data from MR and CT angiography: a correlative study.** *Cerebrovasc Dis* 2015;39:151–61 CrossRef Medline
11. Gupta A, Mtui EE, Baradaran H, et al. **CT angiographic features of symptom-producing plaque in moderate-grade carotid artery stenosis.** *AJNR Am J Neuroradiol* 2015;36:349–54 CrossRef Medline
12. McLaughlin A, Hinckley PJ, Treiman SM, et al. **Optimal prediction of carotid intraplaque hemorrhage using clinical and lumen imaging markers.** *AJNR Am J Neuroradiol* 2015;36:2360–66 CrossRef Medline
13. Mendes J, Parker DL, McNally S, et al. **Three-dimensional dynamic contrast enhanced imaging of the carotid artery with direct arterial input function measurement.** *Magnetic Reson Med* 2014;72:816–22 CrossRef Medline
14. Sorescu GP, Sykes M, Weiss D, et al. **Bone morphogenic protein 4 produced in endothelial cells by oscillatory shear stress stimulates an inflammatory response.** *J Boil Chem* 2003;278:31128–35 CrossRef Medline
15. Towler DA, Shao JS, Cheng SL, et al. **Osteogenic regulation of vascular calcification.** *Ann N Y Acad Sci* 2006;1068:327–33 CrossRef Medline
16. Wahlgren CM, Zheng W, Shaalan W, et al. **Human carotid plaque calcification and vulnerability: relationship between degree of plaque calcification, fibrous cap inflammatory gene expression and symptomatology.** *Cerebrovasc Dis* 2009;27:193–200 CrossRef Medline
17. Shaalan WE, Cheng H, Gewertz B, et al. **Degree of carotid plaque calcification in relation to symptomatic outcome and plaque inflammation.** *J Vasc Surg* 2004;40:262–69 CrossRef Medline
18. van den Bouwhuijsen QJ, Bos D, Ikram MA, et al. **Coexistence of calcification, intraplaque hemorrhage and lipid core within the asymptomatic atherosclerotic carotid plaque: the Rotterdam Study.** *Cerebrovasc Dis* 2015;39:319–24 CrossRef Medline
19. Freilinger TM, Schindler A, Schmidt C, et al. **Prevalence of nonstenosing, complicated atherosclerotic plaques in cryptogenic stroke.** *JACC Cardiovasc Imaging* 2012;5:397–405 CrossRef Medline
20. Hadley JR, Roberts JA, Goodrich KC, et al. **Relative RF coil performance in carotid imaging.** *Magn Reson Imaging* 2005;23:629–39 CrossRef Medline
21. Zhu DC, Ferguson MS, DeMarco JK. **An optimized 3D inversion recovery prepared fast spoiled gradient recalled sequence for carotid plaque hemorrhage imaging at 3.0 T.** *Magn Reson Imaging* 2008;26:1360–66 CrossRef Medline
22. **North American Symptomatic Carotid Endarterectomy Trial: methods, patient characteristics, and progress.** *Stroke* 1991;22:711–20 CrossRef Medline
23. Fox AJ. **How to measure carotid stenosis.** *Radiology* 1993;186:316–18 CrossRef Medline
24. Fox AJ, Eliasziw M, Rothwell PM, et al. **Identification, prognosis, and management of patients with carotid artery near occlusion.** *AJNR Am J Neuroradiol* 2005;26:2086–94 Medline
25. Bartlett ES, Walters TD, Symons SP, et al. **Quantification of carotid stenosis on CT angiography.** *AJNR Am J Neuroradiol* 2006;27:13–19 Medline
26. Menon BK, Singh J, Al-Khataami A, et al; Calgary CTA Study Group. **The donut sign on CT angiography: an indicator of reversible intraluminal carotid thrombus?** *Neuroradiology* 2010;52:1055–56 CrossRef Medline
27. Trelles M, Eberhardt KM, Buchholz M, et al. **CTA for screening of complicated atherosclerotic carotid plaque—American Heart Association type VI lesions as defined by MRI.** *AJNR Am J Neuroradiol* 2013;34:2331–37 CrossRef Medline
28. Zou GY, Donner A. **Extension of the modified Poisson regression**

model to prospective studies with correlated binary data. *Stat Methods Med Res* 2013;22:661–70 CrossRef Medline

29. Maldonado G, Greenland S. **Simulation study of confounder-selection strategies.** *Am J Epidemiol* 1993;138:923–36 Medline

30. Vittinghoff E, McCulloch CE. **Relaxing the rule of ten events per variable in logistic and Cox regression.** *Am J Epidemiol* 2007;165:710–18 CrossRef Medline

31. Pepe M, Longton G, Janes H. **Estimation and comparison of receiver operating characteristic curves.** *Stata J* 2009;9:1 Medline

32. Harrell FE Jr, Lee KL, Mark DB. **Multivariable prognostic models: issues in developing models, evaluating assumptions and adequacy, and measuring and reducing errors.** *Stat Med* 1996;15:361–87 Medline

33. Cheng C, Tempel D, van Haperen R, et al. **Atherosclerotic lesion size and vulnerability are determined by patterns of fluid shear stress.** *Circulation* 2006;113:2744–53 CrossRef Medline

34. Li M, Wu P, Shao J, et al. **Losartan inhibits vascular calcification by suppressing the BMP2 and Runx2 expression in rats in vivo.** *Cardiovasc Toxicol* 2016;16:172–81 CrossRef Medline

35. Takaya N, Yuan C, Chu B, et al. **Presence of intraplaque hemorrhage stimulates progression of carotid atherosclerotic plaques: a high-resolution magnetic resonance imaging study.** *Circulation* 2005;111:2768–75 CrossRef Medline

36. Sun J, Underhill HR, Hippe DS, et al. **Sustained acceleration in carotid atherosclerotic plaque progression with intraplaque hemorrhage: a long-term time course study.** *JACC Cardiovasc Imaging* 2012;5:798–804 CrossRef Medline

37. Underhill HR, Yuan C, Yarnykh VL, et al. **Arterial remodeling in [corrected] subclinical carotid artery disease.** *JACC Cardiovasc Imaging* 2009;2:1381–89 CrossRef Medline

38. Yamada N, Higashi M, Otsubo R, et al. **Association between signal hyperintensity on T1-weighted MR imaging of carotid plaques and ipsilateral ischemic events.** *AJNR Am J Neuroradiol* 2007;28:287–92 Medline